Valence-bond entanglement entropy of frustrated spin chains

Fabien Alet,[1,2] Ian P. McCulloch,[3] Sylvain Capponi,[1,2] and Matthieu Mambrini[1,2]

[1]*Laboratoire de Physique Théorique, IRSAMC, Université de Toulouse–UPS, F-31062 Toulouse, France*

[2]*LPT (IRSAMC), CNRS, F-31062 Toulouse, France*

[3]*School of Physical Sciences, The University of Queensland, Brisbane, Queensland 4072, Australia*

We extend the definition of the recently introduced valence-bond entanglement entropy to arbitrary SU(2) wave functions of $S=1/2$ spin systems. Thanks to a reformulation of this entanglement measure in terms of a projection, we are able to compute it with various numerical techniques for *frustrated* spin models. We provide extensive numerical data for the one-dimensional J_1-J_2 spin chain where we are able to locate the quantum phase transition by using the scaling of this entropy with the block size. We also systematically compare with the scaling of the von Neumann entanglement entropy. We finally underline that the valence-bond entropy definition does depend on the choice of bipartition so that, for frustrated models, a "good" bipartition should be chosen, for instance, according to the Marshall sign.

I. INTRODUCTION

Entanglement is a fundamental notion of quantum mechanics, that has over the recent years gained popularity as a way to provide new insights in the quantum many-body problem. From the condensed-matter point of view, one of the most interesting promises of the study of entanglement properties is the possibility to automatically detect the nature of quantum phases and of quantum phase transitions. In this approach, there is no need to provide *a priori* physical information or input, such as the specification of an order parameter. The detection can occur through the study of the scaling (with system size) of various entanglement estimators. For instance, the scaling of the von Neumann entanglement entropy for one-dimensional (1D) systems is different for critical and gapped systems—allowing their distinction. For a recent review of various properties of entanglement entropy in condenser matter, see Ref. 1.

To quantify the entanglement between two parts Ω and $\bar{\Omega}$ of a quantum system described by a wave function $|\Psi\rangle$, one usually invokes the von Neumann entanglement entropy (vNEE) defined as

$$S^{\text{vN}}(\Omega) = -\text{Tr}_{\Omega}[\hat{\rho}_{\Omega}\ln(\hat{\rho}_{\Omega})],$$

where $\hat{\rho}_{\Omega} = \text{Tr}_{\bar{\Omega}}|\Psi\rangle\langle\Psi|$ is the reduced density matrix obtained by tracing out the degrees of freedom in $\bar{\Omega}$. Considering that Ω is a connected region of space (such as a block of sites in a lattice model), on general grounds one expects that S^{vN} scales not as the volume of Ω, but rather as the interface between Ω and $\bar{\Omega}$. This "area law"[2] is due to the fact that the value of S^{vN} is independent of whether degrees of freedom in Ω or $\bar{\Omega}$ have been first traced out: $S^{\text{vN}}(\Omega) = S^{\text{vN}}(\bar{\Omega})$ and therefore the size dependence must come from the boundary between the two parts of the system.

This general area law has been shown to be fulfilled for many physical wave functions. However it is also known to be violated for several examples, where in most cases some type of long-range correlations develop between degrees of freedom in Ω and $\bar{\Omega}$. The most documented situation is the

case of 1D quantum critical systems where several important results can be derived from conformal field theory (CFT). For 1D quantum critical wave functions displaying conformal invariance, it was shown[3] that $S^{\text{vN}} = \frac{c}{3}\ln(x)$, where x is the length of the block of sites Ω. Here c is the central charge of the corresponding CFT and periodic boundary conditions are assumed. The 1D area law (where S^{vN} saturates to a constant for large x) is fulfilled on the other hand as soon as the correlation length is finite.

Even though one expects the area law to be valid in most cases, the situation of corrections to the area law is still unclear in higher dimensions. CFT predictions are valid only in a few isolated situations.[4,5] Some exact results are available for a few specific models: for instance, the ground-state of free bosonic models fulfills strictly the area law[6,7] whereas free fermions can display multiplicative log corrections.[7,8] On the other hand, calculations for interacting models become rapidly untractable. Numerical simulations are also not eased by the higher dimensionality. Exact diagonalization techniques have access to the vNEE, but they are limited to very small samples sizes which do not allow a test of the area law, and deviations thereof, in high dimension. The vNEE comes for free within the Density Matrix Renormalization Group (DMRG) method[9] but it is limited to 1D and quasi-1D systems. Stochastic methods, such as quantum Monte Carlo (QMC), have no problem with simulations of systems in higher dimensions, but unfortunately the vNEE is a quantity that is extremely complex to measure within Monte Carlo methods (see however recent progresses[10,11]).

Alternatively, it is possible to define for certain quantum spin systems, a different quantifier of entanglement through the use of the valence-bond (VB) representation. The key idea is that for two quantum spins 1/2 at sites i and j, the singlet state (or VB) $|\Psi\rangle = \frac{1}{\sqrt{2}}(|\uparrow_i\downarrow_j\rangle - |\downarrow_i\uparrow_j\rangle)$ is maximally entangled. It can therefore be used as a natural unit of entanglement (in the quantum information community, the entanglement is often measured in units of singlets). Consider now a VB state where an even number N of spins 1/2 are coupled pairwise in singlets, and divide the spins in two arbitrary sets Ω and $\bar{\Omega}$. It is simple to see that the von Neumann entropy

S^{vN} is equal to the number of VBs shared between Ω and $\bar{\Omega}$ (i.e., where one of the two spins is located in Ω and the other in $\bar{\Omega}$), times the constant ln(2). This constant is just the von Neumann entropy of a single spin in a VB. In other words, every singlet that crosses the boundary between Ω and $\bar{\Omega}$ contributes ln(2) to the von Neumann entropy. The picture is very appealing as it provides a simple geometrical interpretation of entanglement, a quantity which is not always easy to grasp intuitively. This argument of course is only exact for the case of VB states, which are simple factorized states. However, it can be shown, and we will describe this in detail below, that the picture holds for all singlet states. This is an important property as most antiferromagnetic systems have a singlet finite-size ground state.

In general, the resulting valence-bond entanglement entropy (VBEE)[12,13] is *different* from the von Neumann entropy, except for the case of VB states where they coincide. There are however several points of interest for this alternative description: (i) it fulfills all desired properties of an entropy,[12] (ii) the VBEE can be easily computed through QMC methods in the VB basis,[14] offering the possibility to study $D > 1$ systems, and (iii) the scaling properties of the VBEE display several interesting features.

Concerning the scaling (with system size) of the VBEE, it has been shown first numerically and then analytically that for critical systems in 1D, the VBEE scales logarithmically with block size $S^{\text{VB}} \propto \gamma \ln(x)$ (here and in the following the symbol $\propto$ denotes proportionality up to a constant). On the other hand, S^{VB} converges to a constant for gapped systems. The same scaling behavior is displayed by the vNEE. The only difference comes from the prefactor of the log divergence: while the numerical estimation of γ was first reported[12] to be consistent with $c/3$ (as for vNEE), the analytical results of Ref. 15 indicate that the two quantities are different for Heisenberg spin chains $\gamma = 4 \ln(2)/\pi^2 \neq 1/3$, even though the numerical value of $\gamma \simeq 0.279$ is very close to 1/3 ($c = 1$ for the Heisenberg chain). We will comment on the numerical validation of the exact value $\gamma = 4 \ln(2)/\pi^2$ at a later stage of this paper.

In two dimensions (2D), the situation seems slightly different. For gapped spins systems, the VBEE was shown[12,13] to fulfill a strict area law $S^{\text{VB}} \propto x$ (with x the linear size of the boundary between Ω and $\bar{\Omega}$). The same scaling is expected on general grounds for S^{vN}. In the case of the ground-state of the two-dimensional Heisenberg model displaying Néel order with gapless excitations, the VBEE displays a multiplicative logarithmic correction to the area law:[12,13,16] $S^{\text{VB}} \propto x \ln(x)$. There is no equivalent calculation (analytical or numerical) for the vNEE of the 2D Heisenberg model, for the reasons described above. However, recent DMRG calculations[16] on N-leg ladders and QMC computations of the Renyi entropy of the 2D Heisenberg model,[17] suggest that the vNEE displays no such multiplicative logarithmic and that the Néel ground state fulfills strictly an area law $S^{\text{vN}} \propto x$. This can be seen negatively as the scaling of the VBEE does not match the one of the vNEE, showing its limits to discuss the adherence of the vNEE to the area law in higher dimensions. One should note however that the VBEE is able to distinguish between a gapless and a gapful

state through its scaling, whereas the vNEE cannot, one of the main original and practical motivations of studying entanglement in condensed-matter systems. As a side remark, we also note that the VBEE can be used to characterize shared information in the different context of stationary states of stochastic models.[18]

In this paper, we investigate the properties of the VBEE using a different approach. The original VBEE definition[12] is intimately related to the fact it is possible to consistently define[19] a VB occupation number able to quantify the presence/absence of a SU(2) dimer on a given bond for any singlet state. Note that the definition only depends on the chosen bipartition of the lattice into two subsets, in spite of the VB basis overcompleteness. We derive in Sec. II an alternative but equivalent definition of the VB occupation number which is free of any VB basis formulation. This allows to define the VBEE in the practical S_z basis and its computation through different numerical schemes [such as exact diagonalization (ED) or DMRG] than the VB QMC method used in previous works. Being now able to compute the VBEE for frustrated systems, we study in Sec. III both vNEE and VBEE for the J_1-J_2 spin chain, using DMRG techniques. We discuss and compare how the scaling of both entropies can detect the critical phase (for small J_2) and the quantum critical point that separates it from the dimerized gapped phase present at large J_2. We also discuss the importance of the Marshall sign present in the ground-state wave function when comparing the two entropies. We finish with a discussion in Sec. IV on the usefulness of the approach, as well as on the further possibilities open by the S_z representation of VB occupation numbers.

II. VB FREE FORMULATION OF THE VBEE

A. VB occupation number as a projection

Original formulation. In this paragraph we recall some definitions and results on VB occupation number.[19] Choosing a bipartition of the N-site lattice into two equal sized subsets $\mathcal{A}$ and $\mathcal{B}$, the bipartite VB subspace is generated by all the bipartite VB states,

$$|\varphi_{\mathcal{D}}\rangle = \bigotimes_{\substack{(i,j) \in \mathcal{D} \\ i \in \mathcal{A}, j \in \mathcal{B}}} [i,j], \tag{1}$$

where $[i,j]$ is a SU(2) dimer state and $\mathcal{D}$ is a dimer covering of the system. For any bond (i,j) such as $i \in \mathcal{A}$ and $j \in \mathcal{B}$ the VB occupation number in the state $|\varphi_{\mathcal{D}}\rangle$ is defined as

$$n_{(i,j)}(|\varphi_{\mathcal{D}}\rangle) = \begin{cases} 1 & \text{if } (i,j) \text{ belongs to } \mathcal{D}, \\ 0 & \text{otherwise.} \end{cases} \tag{2}$$

The bipartite VB manifold is overcomplete: all bipartite VB states are singlet ($S=0$) states but their number $(N/2)!$ is much larger than the singlet subspace dimension.[19,20] As a consequence, a given linear combination of bipartite VB states $|\Psi\rangle = \Sigma_{\mathcal{D}} \lambda_{\mathcal{D}} |\varphi_{\mathcal{D}}\rangle$ can be rewritten in many alternative linear combinations $|\Psi\rangle = \Sigma_{\mathcal{D}} \mu_{\mathcal{D}} |\varphi_{\mathcal{D}}\rangle$ with $\lambda_{\mathcal{D}} \neq \mu_{\mathcal{D}}$. This point requires to reconsider the extension of Eq. (2) for linear combinations of bipartite VB states since the identity

$\Sigma_{\mathcal{D}}\lambda_{\mathcal{D}}n_{(i,j)}(|\varphi_{\mathcal{D}}\rangle)=\Sigma_{\mathcal{D}}\mu_{\mathcal{D}}n_{(i,j)}(|\varphi_{\mathcal{D}}\rangle)$ is not obviously granted. It is nevertheless possible to prove that $n_{(i,j)}$ is linear[19] in $|\varphi_{\mathcal{D}}\rangle$ which provides an intrinsic definition of $n_{(i,j)}(|\Psi\rangle)$ despite the bipartite VB manifold overcompleteness.

Projection (VB states). We give here an alternative but equivalent definition of the VB occupation number which (i) is explicitly independent of the way the state is decomposed in the overcomplete bipartite VB basis, (ii) is valid for any spin S, and (iii) will be shown to be more versatile for numerical computations. The spin-S dimer is defined as the two-site singlet state,

$$[i,j]_S = \frac{1}{\sqrt{2S+1}} \sum_{s_z=-S}^{+S} (-1)^{S-s_z}|-s_z, +s_z\rangle. \qquad (3)$$

We define the reference state

$$|R_S\rangle = |-S, +S, \ldots, -S, +S\rangle, \qquad (4)$$

where the state is written in the $\otimes_i \hat{S}_z$ eigenstates basis and ordered such as $\mathcal{A}$ and $\mathcal{B}$ sites appear in alternating order. In particular, $|R_{1/2}\rangle$ is nothing but the Néel state. As already noticed[14] for $S=1/2$, the reference state has an equal overlap with all bipartite VB states: $\langle R_S|\varphi_{\mathcal{D}}\rangle$ does not depend on the bipartite dimer covering $\mathcal{D}$. This property is established by a direct evaluation from Eqs. (3) and (4) showing $\langle R_S|\varphi_{\mathcal{D}}\rangle = 1/(2S+1)^{N/4}$.

For any bipartite VB state $|\varphi_{\mathcal{D}}\rangle$ and for any bond (i,j) such as $i\in\mathcal{A}$ and $j\in\mathcal{B}$ we are going to show that

$$n_{(i,j)}(|\varphi_{\mathcal{D}}\rangle) = -\frac{(2S+1)^{N/4}}{2S}\langle R_S|\hat{S}_i^+\hat{S}_j^-|\varphi_{\mathcal{D}}\rangle. \qquad (5)$$

Indeed, we have

$$\hat{S}_i^+\hat{S}_j^-|R_S\rangle = (2S)|\ldots, \overbrace{-S+1}^{i}, \overbrace{S-1}^{j}, \ldots\rangle. \qquad (6)$$

If the bond (i,j) is occupied, $|\varphi_{\mathcal{D}}\rangle = \cdots \otimes [i,j]_S \otimes \cdots$ and a simple inspection of Eq. (3) shows that $\langle R_S|\hat{S}_i^+\hat{S}_j^-|\varphi_{\mathcal{D}}\rangle = -(2S)/(2S+1)^{N/4}$ and hence $n_{(i,j)}(|\varphi_{\mathcal{D}}\rangle)$ as defined in Eq. (5) is 1. On the other hand, $|\varphi_{\mathcal{D}}\rangle = \cdots \otimes [i,k]_S \otimes [l,j]_S \cdots$ if the bond (i,j) is unoccupied. The total S_z component on any occupied bond of a VB state is 0. Thus any eigenstate of $\hat{S}_i^z + \hat{S}_k^z$ (or $\hat{S}_l^z + \hat{S}_j^z$) with a nonzero eigenvalue is then orthogonal to $|\varphi_{\mathcal{D}}\rangle$. It is salient from Eq. (6) that $(\hat{S}_i^z + \hat{S}_k^z)\hat{S}_i^+\hat{S}_j^-|R_S\rangle = +\hat{S}_i^+\hat{S}_j^-|R_S\rangle$ and $(\hat{S}_l^z + \hat{S}_j^z)\hat{S}_i^+\hat{S}_j^-|R_S\rangle = -\hat{S}_i^+\hat{S}_j^-|R_S\rangle$. Hence $n_{(i,j)}(|\varphi_{\mathcal{D}}\rangle)$ as defined in Eq. (5) is 0 in this case.

Finally, it is easy to see that if both i and j sites are located in the same subset $\mathcal{A}$ or $\mathcal{B}$, the definition Eq. (5) also ensures that $n_{(i,j)}=0$ which is always true (independently of $|\varphi_{\mathcal{D}}\rangle$) as no dimer is allowed on such a nonbipartite bond. Let us mention some of the advantages of definition Eq. (5) as an alternative to Eq. (2). First of all, it is explicitly linear in $|\varphi_{\mathcal{D}}\rangle$ which ensures that its extension to arbitrary linear combination of bipartite VB states can be consistently defined. As stated before, in the case of $S=1/2$, the subspace of bipartite VB states is a basis of the total singlet sector, ensuring that a dimer occupation number can be defined for any $S=1/2$ singlet. This is not true anymore for general spin

S: bipartite spin-S VB states do not form a basis of spin-S singlets. However it can be shown that they form a basis of the subset of spin-S singlets that are also SU(N) singlets[21] (with $N=2S+1$) so that Eq. (5) can be useful in that context.

Projection (VB states superpositions). Using Eq. (5), the occupation number for an arbitrary linear combination of bipartite VB states $|\Psi\rangle = \Sigma_{\mathcal{D}}\lambda_{\mathcal{D}}|\varphi_{\mathcal{D}}\rangle$ is defined as

$$n_{(i,j)}(|\Psi\rangle) = -\mathcal{N}\frac{(2S+1)^{N/4}}{2S}\langle R_S|\hat{S}_i^+\hat{S}_j^-|\Psi\rangle, \qquad (7)$$

where $\mathcal{N}$ is a normalization constant. It would be tempting to take $\mathcal{N}=1/\sqrt{\langle\Psi|\Psi\rangle}$. However $n_{(i,j)}$ is designed to measure the number of dimers (0 or 1) on bond (i,j) and for any VB state a given site $i\in\mathcal{A}$ is dimerized with another site on sublattice $\mathcal{B}$. Hence the normalization condition writes

$$\sum_{j\in\mathcal{B}} n_{(i,j)}(|\Psi\rangle) = 1. \qquad (8)$$

This condition enforces

$$\mathcal{N} = \frac{1}{\sum_{\mathcal{D}} \lambda_{\mathcal{D}}} = \frac{1}{(2S+1)^{N/4}\langle R_S|\Psi\rangle} \qquad (9)$$

and

$$n_{(i,j)}(|\Psi\rangle) = -\frac{1}{2S}\frac{\langle R_S|\hat{S}_i^+\hat{S}_j^-|\Psi\rangle}{\langle R_S|\Psi\rangle}. \qquad (10)$$

Contrary to Eq. (2), this last expression is *explicitly independent* of the linear combination chosen to expand $|\Psi\rangle$ on the overcomplete bipartite VB manifold as it only involves projections of $|\Psi\rangle$. Since Eq. (7) does not give any prominent role to the bipartite VB basis to express $|\Psi\rangle$, it will allow numerical computations outside the VB QMC scheme such as with exact diagonalization and DMRG (see Sec. II B).

Note that this expression is potentially singular if $|R_S\rangle$ is orthogonal to $|\Psi\rangle$. As an example, let us consider a one-dimensional spin-1/2 chain with $N=4p$ sites (where p is an integer). If we denote $\mathcal{S}$ the spin inversion symmetry $S^z \to -S^z$ and $\mathcal{T}$ the translation symmetry, any $q=\pi$ singlet state $|\Psi\rangle$ will transform as $\mathcal{S}|\Psi\rangle=|\Psi\rangle$ and $\mathcal{T}|\Psi\rangle=-|\Psi\rangle$. Consequently, $\mathcal{ST}|\Psi\rangle=-|\Psi\rangle$. On the other hand, if the bipartition $\mathcal{ABAB}\ldots$ is chosen, the reference state given in Eq. (4) is obviously invariant under $\mathcal{ST}$. As a consequence, $|\Psi\rangle$ and $|R_S\rangle$ are orthogonal and Eq. (10) cannot be used.

This issue, which is a direct consequence of the normalization defined by Eq. (9), suggests that the bipartition and hence $|R_S\rangle$ [see Eq. (4)] may not be chosen regardless of $|\Psi\rangle$. More generally, normalizing a state by the sum of its coefficients in an expansion like in Eq. (9), requires a careful inspection of its nodal structure or equivalently of its Marshall sign which in turn dictates an appropriate bipartition for the reference state. We will further discuss this issue in Sec. III C.

VBEE. Using Eq. (10), the VBEE measuring the entanglement between Ω or $\bar{\Omega}$ in a state $|\Psi\rangle$ can be expressed as
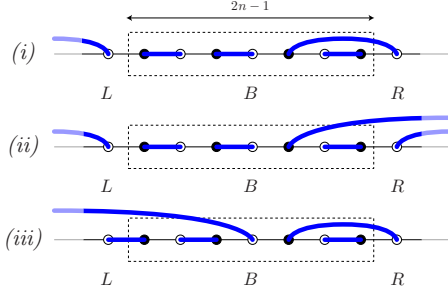
FIG. 1. (Color online) Three possible cases for valence-bond configurations in the noncrossing basis for a given block B with an odd number of sites and neighboring sites L and R (see text for details).

$$S_\Omega^{\text{VB}}(|\Psi\rangle) = \ln 2 \times \sum_{\substack{(i,j) \text{ such as} \\ i\in\Omega, j\in\bar{\Omega}}} n_{(i,j)}(|\Psi\rangle), \qquad (11)$$

where the spatial sums run over all possible locations of VBs, that is over all sites i in Ω and all sites j in $\bar{\Omega}$. Since we know that $n_{(i,j)}=0$ whenever i and j belong to the same subset $\mathcal{A}$ or $\mathcal{B}$, we can restrict the summation only to the nonvanishing cases.

VBEE for one-dimensional periodic systems. We finally make a remark on the behavior of S_Ω^{VB} for translation-invariant one-dimensional systems. When Ω is a linear segment of size $2n$ (with n integer) we find that

$$S^{\text{VB}}(2n) = \frac{1}{2}[S^{\text{VB}}(2n-1) + S^{\text{VB}}(2n+1)], \qquad (12)$$

which means graphically that S^{VB} is made of linear segments. Let us propose an easy graphical proof of this statement. Consider a VB configuration and let us compare VBEE for different blocks obtained by adding two extra sites R and L at each end of a $(2n-1)$-sites block B (see Fig. 1). Since the VBEE is a well-defined quantity, we can choose to work in the complete noncrossing basis[20] where VB do not cross according to some one-dimensional ordering of the sites. Since the $2n-1$ block has an odd number of sites, it is clear that R and L *cannot* be connected by a singlet. Then, we can consider all possible cases: (i) R is connected to B but not L, or vice versa; (ii) neither R nor L are connected to B; and (iii) both R and L are connected with B. These cases are shown in Fig. 1 and from the figure, it is straightforward to check that $S^{\text{VB}}(B) + S^{\text{VB}}(B+R+L) = S^{\text{VB}}(B+R) + S^{\text{VB}}(B+L)$. As a conclusion, if periodic boundary conditions are used so that the entropy only depends on the number of sites of the block, we deduce Eq. (12).

B. Numerical computations

From now on, we focus on the case of $S=1/2$ systems.

With exact diagonalization. We use the Lanczos algorithm in order to compute the ground state of large 1D chains.[22] We also implement lattice translations as well as fixing the total S^z quantum number in order to reduce the Hilbert space size so that we can solve systems up to $N=32$ sites. Once the

wave function is obtained in the symmetrized basis, one can easily compute its overlap with the reference state, which gives the denominator of Eq. (10). In order to compute its numerator, we need to apply the operator $\hat{S}_i^+\hat{S}_j^-$ for all pairs of sites (i,j) with i in the selected block and j outside (let us remind that we can restrict ourselves to the case where i and j belong to different subsets). In this case, it turns out that it is simpler to apply this spin operator on the reference state since it reduces to a swap operator for spins 1/2. Finally, in order to compute the VBEE, and since we are using translation symmetry, we have to make an average over all the positions of the block on the chain.

With DMRG, The calculation of the VB entanglement entropy is straightforward, utilizing matrix product techniques to calculate the overlap between the ground state and the reference state $N = \langle\uparrow\downarrow\uparrow\cdots\downarrow|\Psi\rangle$, and the expectation value $P = \langle\uparrow\downarrow\uparrow\cdots\downarrow|\mathcal{P}|\Psi\rangle$, where $\mathcal{P} = \Sigma_{i\in\Omega, j\in\bar{\Omega}} S_i^+ S_j^- + S_j^+ S_i^-$ has a simple representation as a matrix product operator, using the techniques described in Ref. 23. The VB entanglement entropy is then $S^{\text{VB}} = -\ln(2)P/N$.

III. RESULTS FOR THE J_1-J_2 SPIN CHAIN

A. Model and simulation details

We now present numerical results for the frustrated J_1-J_2 spin chain. $|\Psi\rangle$ in Eq. (11) is taken as the ground state of the $S=1/2$ Hamiltonian,

$$H = \sum_{i=1}^{L} J_1 \mathbf{S}_i \cdot \mathbf{S}_{i+1} + J_2 \mathbf{S}_i \cdot \mathbf{S}_{i+2}, \qquad (13)$$

where we set $J_1=1$ and will vary J_2. The physics of this spin chain is well understood: for J_2 smaller than the critical value $J_2^c \simeq 0.241167$ (Ref. 24), the system displays antiferromagnetic quasilong-range order, with algebraically decaying spin correlations. For $J_2 > J_2^c$, the system is located in a gapped dimerized phase which spontaneously breaks translation symmetry. We will study both VBEE and vNEE entropies in this system in both phases.

Results for $J_2 \leq 0.5$ were obtained with DMRG. We used samples with $L=64$, 128, and 192 and periodic boundary conditions in order to avoid dimerization effects in the entanglement entropy,[12,25] which complicate the finite-size analysis. Up to $m=1092$ SU(2) states [roughly corresponding to 4000 usual U(1) states] have been kept for the largest samples. A long warm-up procedure has been used, by performing between 10 and 50 sweeps each time m was increased by 50. Convergence has been checked by ensuring that the energy does not change significantly on more than 20 sweeps for the last value of m. Truncation error per site and variance per site $(H-E)^2/L$ were always at most 10^{-10} for the largest systems. For these periodic boundary conditions, a two-sites version of the DMRG algorithm has been used. We will essentially present results for the largest $L=192$ chains but will occasionally show data for smaller L when a discussion of finite-size effects is necessary.

Prior to calculating the scalar products with the reference state, we use the Wigner-Eckart theorem to project the SU(2)
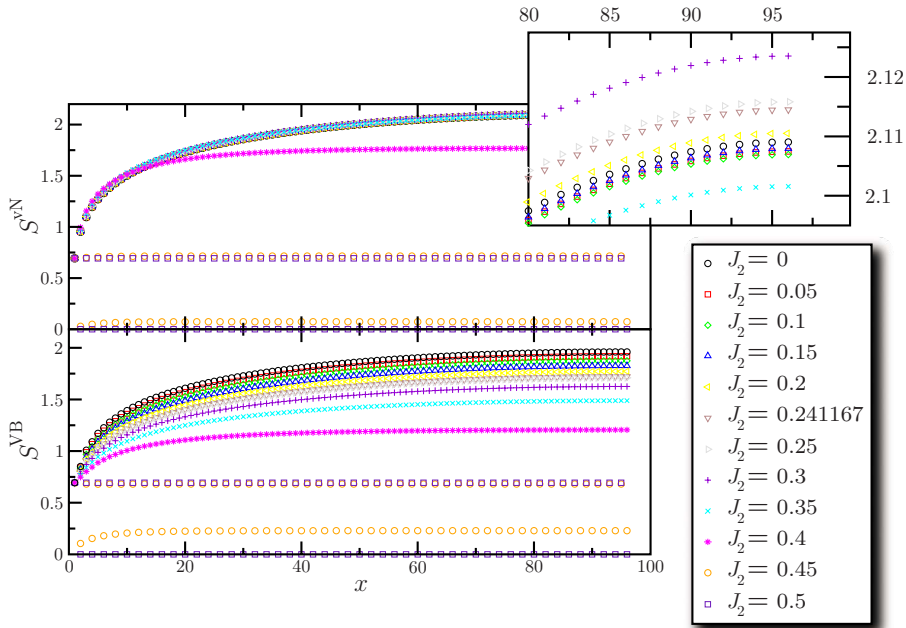
FIG. 2. (Color online) Scaling of von Neumann S^{vN} (top panel) and valence-bond S^{VB} (bottom panel) entanglement entropies as a function of block size x, for different values of the frustrating coupling J_2. Chain length is $L=192$. Top inset is a zoom of S^{vN} for x close to $L/2$.

ground state to U(1), thus giving direct access to the axis-dependent spin vector operators. Later in the paper, we will present results for $J_2 > 0.5$ which were obtained with ED for chains of length up to $L=32$. For large values of J_2, the DMRG algorithm has more difficulties to converge, even for small samples—a fact which has already been reported.[26] Also, some intrinsic difference shows up in the definition of the VBEE in this case due to the rapid vanishing of the Marshall sign in the ground-state wave function. In that situation, the analysis of the definition as well as meaning of the VBEE is different and will be discussed in Sec. III C.

We finally note that the vNEE of the ground state of this spin chain was studied previously,[27] albeit on smaller systems, with ED techniques. As we will see later, the use of large systems is necessary to locate precisely the quantum phase transition at J_2^c.

B. Results for $J_2 \leq 0.5$

We will present in this section results obtained for vNEE and VBEE entanglement entropies in parallel. We first present raw data for both entropies as a function of the block size x for different values of J_2 in Fig. 2. Data are shown only for $x \in [0, L/2]$ (we have checked that curves are symmetric around $L/2$). Both sets of curves show a similar behavior: on the scale of the figure, one can distinguish between curves which converge to a constant (for $J_2 \geq 0.4$) and those which grow slowly but steadily with x. The difference between the two entropies appears on the former cases, where curves for different J_2 appear more shifted for S^{VB}. The shift also exists for S^{vN} but is smaller (see zoom around $x \sim L/2$ in the inset of the figure).

One should also note the clear dimerization of both entropies for large J_2: this is naturally expected at the Majumdar-Ghosh[28] point $J_2 = 1/2$ where S^{VB} and S^{vN} are strictly equal to 0 for even x and $\ln(2)$ for odd x. Note that this dimerization effect comes from the intrinsic dimerized nature of the ground state in this region and not from the boundary conditions as in Ref. 25.

Let us concentrate now on the upper beam of curves for $J_2 \leq 0.35$. From conformal invariance of the ground state in the critical phase, the use of the conformal block length $x' = L/\pi \sin(\pi x/L)$ should be useful for systems with periodic boundary conditions: in the critical phase, vNEE should scale as $S^{vN} = c/3 \ln(x') + K_1$ whereas $S^{VB} = \gamma \ln(x') + K_2$.

Figure 3 displays both entropies versus x' in a log-linear scale. All curves seem at first glance linear with approximately the same slope, except for $J_2 = 0.35$ where a crossover to a constant regime can be identified: this is well visible for S^{vN} in the figure, but is also the case for S^{VB} when zoomed in.

We fit the curves to a form $S^{vN} = c_{\rm eff}/3 \ln(x') + K_1$ and $S^{VB} = \gamma_{\rm eff} \ln(x') + K_2$ within the window $x' > 10$. Fits are excellent and lead to $c_{\rm eff}$ (respectively, $\gamma_{\rm eff}$) very close to the CFT prediction 1 [respectively, $4 \ln(2)/\pi^2$] in the critical phase. The values of the fitted $c_{\rm eff}$ and $\gamma_{\rm eff}$ are displayed in the left insets of Fig. 3, as obtained for the three different samples sizes L used in this study. The finite-size effects are found to be small on both quantities.

Several remarks are in order at this stage: (i) the finite-size dependence of the fitted values indicate that $J_2 = 0.35$ is clearly not in the critical regime as we already guessed from a visual inspection of curves. (ii) It is quite interesting to note that both $\gamma_{\rm eff}$ and $c_{\rm eff}$ are not strictly equal to the predicted values for low J_2 (including $J_2 = 0$) but are getting closer monotonously to the theoretical predictions when increasing J_2. This effect can clearly be seen for $\gamma_{\rm eff}$ but also exist (even if small) for $c_{\rm eff}$. (iii) The values closest to 1 and $4 \ln(2)/\pi^2$ are found to be precisely at $J_2^c = 0.241167$. The fitted $c_{\rm eff}$ is smaller than 1 for $J_2 = 0.30$ and $\gamma_{\rm eff}$ is smaller than $4 \ln(2)/\pi^2$ for $J_2 \geq 0.241167$.

The two former points lead to the following interpretation: given the existence of dangerously irrelevant operators in the critical phase (but not at J_2^c), we expect that they could
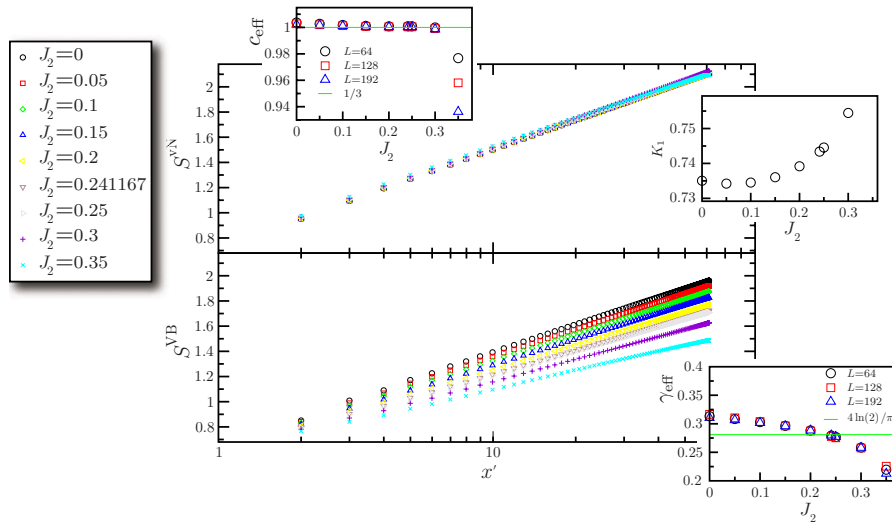
FIG. 3. (Color online) Scaling of von Neumann S^{vN} (top panel) and valence-bond S^{VB} (bottom panel) entanglement entropies as a function of conformal block size $x' = L/\pi \sin(\pi x/L)$ in a log-linear scale, for different values of the frustrating coupling J_2. Chain length is here $L=192$. Top left (bottom right) inset shows the value of the coefficient of a log fit for both von Neumann (valence-bond) entanglement entropies as a function of J_2, for different system sizes (see text for details). Top right inset gives the value of the nonuniversal additive constant K_1 obtained from the same fit of S^{vN}, as a function of J_2 for $L=192$.

influence the effective value of the central charge and γ as measured from a fit of EE on finite systems (they should not in the thermodynamic limit). The strength of their influence decreases as one approaches the critical point where they vanish. This scenario sounds plausible for γ: indeed in the field-theoretical description of the Heisenberg chain, γ is related to the coupling constant of the free boson field whose numerical determination is known to suffer from log corrections due to dangerously irrelevant operators. A similar effect has been recently predicted for the effective central charge in presence of marginally irrelevant operators,[29] with the prediction that $c_{eff} < c$. Raw fits of the form $S^{vN} = c_{eff}/3 \ln(x') + K_1$ appear to give a value of c_{eff} slightly larger than 1 (in all cases less than 1%). We find however that the simultaneous fits of c_{eff} and K_1 actually affect the determination of c_{eff}. A more precise fitting procedure[30] along the lines of Ref. [31] produce values of $c_{eff} < 1$ in agreement with Ref. [29]. Details of such a precise estimation of c_{eff} are left for a future study (we checked that a similar analysis for γ_{eff} does not affect the results displayed in Fig. [3]).

The analysis above explains why first simulations of the unfrustrated Heisenberg chain (at $J_2=0$) indicate that the scaling of the VBEE was identical to the one of vNEE: indeed the fitted value of $\gamma_{eff} \sim 0.310$ is closer to 1/3 than to $4 \ln(2)/\pi^2 \simeq 0.281$. We note that the transfer matrix estimates of γ_{eff} also display such a small discrepancy for the Heisenberg chain.[15] The numerical results of Ref. [15] for other spin chains not suffering from these log corrections appear to be in much better agreement with the analytical predictions, confirming this scenario.

Actually, the vanishing of these log corrections appear as a way to detect on finite systems the quantum critical point J_2^c through the log scaling of S^{VB} (and possibly S^{vN}), as long as the exact values $\gamma = 4 \ln(2)/\pi^2$ and $c=1$ are known. If these values were not available, it would be more difficult to judge on the extent of the critical phase. Indeed from the sole

quality of the fits, data at $J_2=0.25$ and $J_2=0.30$ (which are theoretically located in the gapped phase) are compatible with a critical scaling. This is certainly due to the small simulation length used L with respect to the large correlation length close to J_2^c.

Finally, we discuss the behavior of the constants K_1 and K_2. Both constants are nonuniversal and are *a priori* not related. The fitted value of K_1 is shown in the right inset of Fig. [3] and displays a nonmonotonous behavior (especially at small J_2). This nonmonotonous behavior can also directly be seen on the raw S^{vN} data at $L/2$ (inset of Fig. [2]). On the other hand, and this can be noticed without a fit, the constant K_2 for S^{VB} decreases monotonously with J_2.

The final transformation which summarizes these results consists in directly subtracting the expected exact value from both entanglement entropies. Figure [4] displays $S^{vN} - 1/3 \ln(x')$ and $S^{VB} - \gamma \ln(x')$ versus x'. Curves should saturate to the constants K_1 and K_2, respectively, which they do (except obviously for $J_2=0.35$) on this scale. Zooming in,
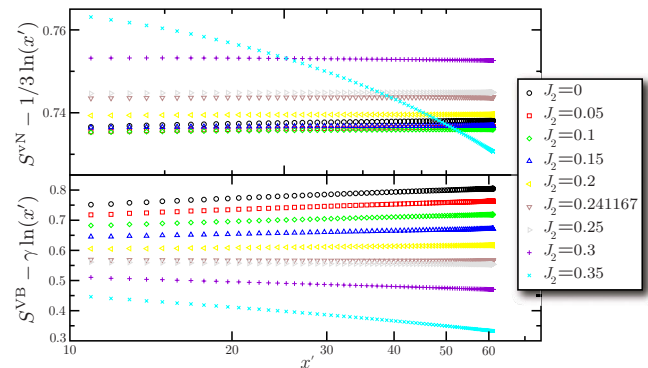

FIG. 4. (Color online) Difference of the entanglement entropies to the predicted analytical values $S^{vN} - 1/3 \ln(x')$ (top panel) and $S^{VB} - \gamma \ln(x')$, as a function of conformal block size x', for different values of the frustrating coupling J_2. Chain length is here $L=192$.
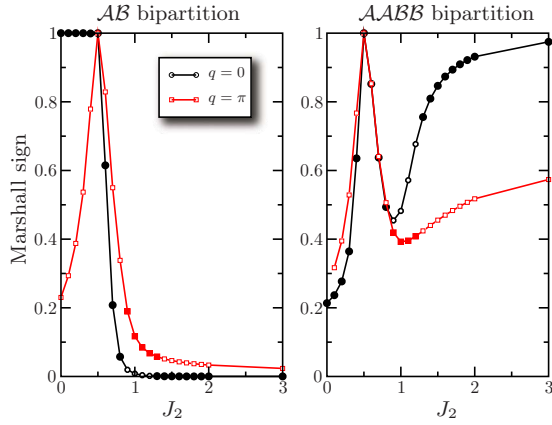
FIG. 5. (Color online) Marshall sign vs J_2 for a $L=32$ chain for both the lowest $q=0$ and $q=\pi$ eigenstates. Left: $\mathcal{AB}$ partition for the Marshall sign. Right: $\mathcal{AABB}$ partition. Ground-state results are denoted with filled symbols.

one observes that all curves for S^{vN} grow in a very smooth way, except for $J_2=0.30$ which actually decreases with x' (for S^{VB}, all curves for $J_2 \geq 0.241167$ tend to decrease when increasing block size x'). This is in correspondence with the fitted $c_{\text{eff}} < 1$ for this value of J_2. The flattest curves are observed for $J_2 = 0.241167 \sim J_2^c$ and $J_2 = 0.25$ for both entropies, in agreement with our previous observations.

C. Results for $J_2 > 0.5$

Knowing the nodes and the signs of all coefficients of a correlated wave function is a difficult task. Indeed, such an information could allow to design a sign-free QMC algorithm as well as help on building variational wave functions. In this context, one can define the so-called Marshall-Peierls sign[32]

$$s(|\Psi\rangle) = \sum_i (-1)^{N_\uparrow^{\mathcal{B}}} a_i |a_i|, \quad (14)$$

where the sum runs over the $|\psi_i\rangle$ $\hat{S}_z$ basis states and with the wave function given by $|\Psi\rangle = \Sigma_i a_i |\psi_i\rangle$. $N_\uparrow^{\mathcal{B}}$ counts the number of up spins on the $\mathcal{B}$ sublattice so that obviously, s depends on the choice of bipartition.

For nonfrustrated Heisenberg model, it can be shown that the ground state has $s=1$ with the natural choice of bipartition.[33] Frustration will spoil this result, although the sign may not drop suddenly (see, for instance, 1D or 2D J_1-J_2 model[34]). On left panel of Fig. 5, we present ED data for the frustrated Heisenberg chain. With the natural $\mathcal{AB}$ bipartition, the Marshall sign stays extremely close to 1 for $0 \leq J_2 \leq 0.5$ but starts to deviate substantially beyond. Since the ground state oscillates between having momentum 0 and π, we plot both values of s.

Figure 6 shows ED data for various entropies. In particular, since S^{VB} depends on the choice of bipartition, one may wonder what to choose. Usually, one is guided by the Ising solution: for small J_2/J_1, it is natural to choose a $\mathcal{ABAB}\ldots$ bipartition, while for large J_2/J_1, the system will behave as two decoupled Heisenberg chains with twice as large lattice
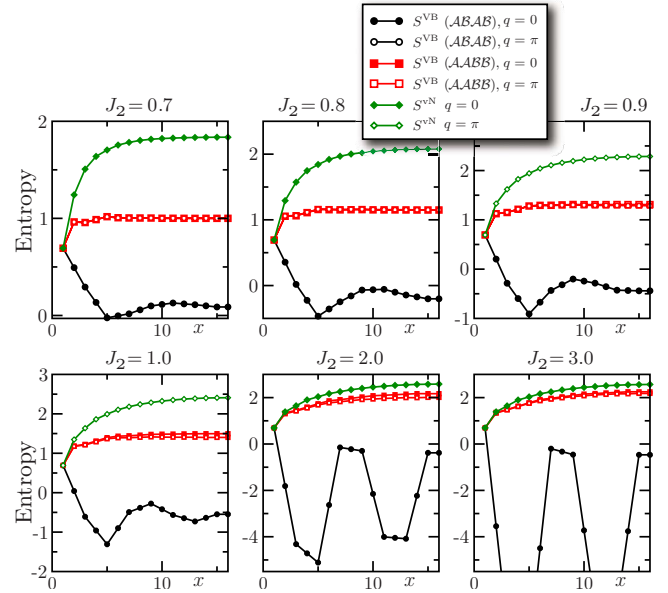

FIG. 6. (Color online) Entropy vs block size for various frustration parameter J_2 on $L=32$ system obtained with ED. Several S^{VB} are plotted for the lowest $q=0$ (filled symbols) and $q=\pi$ (open) eigenstates, and for both choices of bipartition corresponding to Ising configurations for $J_2=0$ ($\mathcal{ABAB}$) and $J_1=0$ ($\mathcal{AABB}$), respectively. S^{vN} is plotted for the ground state.

spacing, meaning that bipartition should be of the form $\mathcal{AABB}\ldots$ The Marshall sign for this $\mathcal{AABB}$ partition is presented in the right panel of Fig. 5.

Of course, the intermediate region with maximal frustration has no preferred bipartition. Moreover, since the ground state oscillates between $q=0$ and $q=\pi$, we plot both entropies. Still, as can be seen from its definition Eq. (11), S^{VB} is only defined when the overlap between the ground state and the classical Néel state is finite. Unfortunately, the $\mathcal{ABAB}$ Néel state has no projection in the singlet $q=\pi$ sector as it is invariant by a combination of lattice translation and spin reversal. However, for $\mathcal{AABB}$ bipartition, we can compute S^{VB} for both lowest $q=0$ and $q=\pi$ states and it turns out that data are very similar (sometimes they cannot be distinguished on the scale of Fig. 6), although states are quite different (see their Marshall sign in Fig. 5).

By comparing Figs. 5 and 6, we observe that when the Marshall sign is too small, S^{VB} has absolutely no meaning (and can even be negative). On the other hand, is s is large enough, or said differently, if we choose the bipartition that maximizes s, then S^{VB} behaves much better and follows the same trend as S^{vN}, that is both entropies converge to a constant for large enough block size. In fact, for large J_2/J_1 where the Marshall sign becomes again close to 1 for the $\mathcal{AABB}$ choice, we observe that both entropies become more and more similar.

IV. DISCUSSION

In this paper, we studied the behavior of the valence-bond entanglement entropy of the frustrated J_1-J_2 spin chain, and offered a direct comparison with the von Neumann entropy.

Numerical DMRG calculations indicate that both entropies scale logarithmically with block size in the critical phase and converge in the gapped dimerized phase of this model. The study of the VBEE has been made possible in this frustrated model through a formulation of valence-bond occupation number, which extends this notion out of the valence-bond basis.

We now discuss several interests of studying entanglement in quantum spin systems through a valence-bond measure and point out some open issues. First, as based on the example of the J_1-J_2 model, the scaling of S^{VB} with the block size allows to differentiate critical from gapped phases in one dimension, similarly to S^{vN}. Moreover, the knowledge of the exact prefactor[15] of the log scaling permits a relatively precise determination of the quantum critical point at J_2^c with finite-size data (this is however due to the vanishing of log corrections at this particular point, a nongeneric feature). Note that this knowledge can be useful as the scaling of S^{VB} might now be used to characterize uniquely the unknown phase of a new model. S^{VB} can be computed for the Q-states Potts model using the loop language of Ref. [15] and there, the prefactor of the logarithmic scaling depends on Q and is therefore indeed different for the different critical points encountered in the Potts model. This is similar to the scaling of S^{vN} which allows the determination of the central charge—the knowledge of which entirely determines the CFT at play for minimal models.

It is possible to compute S^{VB} directly in the thermodynamic limit using the infinite-size versions of DMRG (Ref. [25]) or of time-evolving block decimation (iTEBD).[36] In this formulation, the number of basis states in the calculation controls the spectrum transfer matrix of the system, which gives a scaling of the correlation length $\xi \propto m^\kappa$ at criticality, where κ is a function of the central charge.[37] However, the effective boundary condition for the transfer matrix, and hence the form of the corrections to scaling of the entropies S^{VB} and S^{vN}, will be different to the case of periodic boundary conditions, and we leave this analysis for a future study. Besides, knowing the corrections to scaling induced on a finite system by marginally irrelevant operators is interesting by itself (see, for instance, Ref. [29]).

In dimension higher than 1, it was already demonstrated[12,13,16] that the scaling of S^{VB} discriminates between gapped and gapless phases. Since numerical calculations are possible in $D>1$ with QMC VB methods,[14] it would be of high interest to perform a systematic study of the scaling of S^{VB} in different phases of quantum spin models. Several questions are in order: for instance, do the multiplicative log corrections observed for the 2D Heisenberg model have a physical interpretation? Are prefactors of the scaling of S^{VB} universal within a phase or at a quantum critical point,[13] as observed in 1D?

We note that the techniques described here for calculating the valence-bond entanglement entropy can easily be applied to higher-dimensional tensor network algorithms such as projected entangled-pair states (PEPS) (Ref. [38]) where the necessary scalar products are similarly easily computed. This opens the door to studies of the VBEE for frustrated 2D systems.[39]

Our study on frustrated systems also sheds lights on the importance of a good physical choice for the bipartition used in the definition of the VBEE and its relation to the existence of a Marshall sign rule (or a large Marshall sign) in the wave function under study. When the Marshall sign is exactly or close to 1, the resulting choice of bipartition [or equivalently reference state $|R_S\rangle$ in Eq. (10)] produces a valence-bond entanglement entropy that closely follows the scaling of the von Neumann entropy. This suggests another route to quantify entanglement in a wave function through its projection over a well-chosen (physical) reference state.

Another interesting situation which we have not discussed in this work is the one of strongly disordered spin systems, where S^{VB} and S^{vN} coincide[40] (after averaging over disorder). This is the case in the random singlet phase, where the low-energy physics is dominated by a single valence-bond state, as remarked in Ref. [12] and more recently by Tran and Bonesteel.[41] As pointed out by these authors, the study of the *fluctuations* of the number of VBs crossing the boundary provide additional physical insights in this situation.

Finally, we comment on the usefulness of the formulation Eq. (10) of the valence-bond occupation number. It clearly points toward generalizations of S^{VB} for situations not explored before, for instance, for spins higher than 1/2, as well as for systems which lack SU(2) symmetry. In the latter case, the direct interpretation in terms of SU(2) VBs is not possible anymore and the physical meaning of $n_{(i,j)}$ has first to be clarified. It would be interesting, for instance, to look for the relation to q-deformed singlets,[42] which are used in Ref. [15] to extend the VBEE to Potts models. Another high interest of Eq. (10) is that it allows analytical insights on the distribution of valence bonds and their correlations in a singlet ground state.[43]

[1] P. Calabrese, J. Cardy, and B. Doyon, J. Phys. A **42**, 500301 (2009).

[2] M. Srednicki, Phys. Rev. Lett. **71**, 666 (1993); J. Eisert, M. Cramer, and M. B. Plenio, Rev. Mod. Phys. **82**, 277 (2010).

[3] C. Holzhey, F. Larsen, and F. Wilczek, Nucl. Phys. B **424**, 443 (1994); G. Vidal, J. I. Latorre, E. Rico, and A. Kitaev, Phys. Rev. Lett. **90**, 227902 (2003); J. I. Latorre, E. Rico, and G. Vidal, Quantum Inf. Comput. **4**, 48 (2004); P. Calabrese and J. Cardy, J. Stat. Mech.: Theory Exp. (2004) P06002.

[4] E. Fradkin and J. E. Moore, Phys. Rev. Lett. **97**, 050404 (2006).

[5] J.-M. Stéphan, S. Furukawa, G. Misguich, and V. Pasquier, Phys. Rev. B **80**, 184421 (2009).

[6] M. Cramer, J. Eisert, M. B. Plenio, and J. Dreissig, Phys. Rev. A **73**, 012309 (2006).

[7] T. Barthel, M.-C. Chung, and U. Schollwöck, Phys. Rev. A **74**, 022329 (2006).

[8] M. M. Wolf, Phys. Rev. Lett. **96**, 010404 (2006); D. Gioev and I. Klich, *ibid.* **96**, 100503 (2006).

[9] S. R. White, Phys. Rev. Lett. **69**, 2863 (1992).

[10] P. V. Buividovich and M. I. Polikarpov, Nucl. Phys. B **802**, 458 (2008).

[11] M. Caraglio and F. Gliozzi, J. High Energy Phys.JHEP11, (2008) 076.

[12] F. Alet, S. Capponi, N. Laflorencie, and M. Mambrini, Phys. Rev. Lett. **99**, 117204 (2007).

[13] R. W. Chhajlany, P. Tomczak, and A. Wójcik, Phys. Rev. Lett. **99**, 167204 (2007).

[14] A. W. Sandvik, Phys. Rev. Lett. **95**, 207203 (2005); A. W. Sandvik and H.-G. Evertz, Phys. Rev. B **82**, 024407 (2010).

[15] J. L. Jacobsen and H. Saleur, Phys. Rev. Lett. **100**, 087205 (2008).

[16] A. B. Kallin, I. González, M. B. Hastings, and R. G. Melko, Phys. Rev. Lett. **103**, 117203 (2009).

[17] M. B. Hastings, I. González, A. B. Kallin, and R. G. Melko, Phys. Rev. Lett. **104**, 157201 (2010).

[18] F. C. Alcaraz, V. Rittenberg, and G. Sierra, Phys. Rev. E **80**, 030102(R) (2009); F. C. Alcaraz and V. Rittenberg, J. Stat. Mech.: Theory Exp. (2010) P03024; P. Calabrese, *ibid.* (2010) N05001; A. L. Owczarek, *ibid.* (2009) P12004.

[19] M. Mambrini, Phys. Rev. B **77**, 134430 (2008).

[20] G. Rumer, E. Teller, and H. Weyl, Nachr. Ges. Wiss. Goettingen, Math.-Phys. Kl. No. **5**, 499 (1932); see also H. N. V. Temperley and E. H. Lieb, Proc. R. Soc. London, Ser. A **322**, 251 (1971); and R. Saito, J. Phys. Soc. Jpn. **59**, 482 (1990).

[21] K. S. D. Beach, F. Alet, M. Mambrini, and S. Capponi, Phys.

[22] See, for instance, N. Laflorencie and D. Poilblanc, Lect. Notes Phys. **645**, 227 (2004), and references therein.

[23] I. P. McCulloch, J. Stat. Mech.: Theory Exp. (2007) P10014.

[24] S. Eggert, Phys. Rev. B **54**, R9612 (1996).

[25] N. Laflorencie, E. S. Sørensen, M.-S. Chang, and I. Affleck, Phys. Rev. Lett. **96**, 100603 (2006).

[26] S. R. White and I. Affleck, Phys. Rev. B **54**, 9862 (1996).

[27] R. W. Chhajlany, P. Tomczak, A. Wójcik, and J. Richter, Phys. Rev. A **75**, 032340 (2007).

[28] C. K. Majumdar and D. K. Ghosh, J. Math. Phys. **10**, 1388 (1969); **10**, 1399 (1969).

[29] J. Cardy and P. Calabrese, J. Stat. Mech.: Theory Exp. (2010) P04023.

[30] P. Calabrese (private communication).

[31] J. C. Xavier, Phys. Rev. B **81**, 224404 (2010).

[32] W. Marshall, Proc. R. Soc. London, Ser. A **232**, 48 (1955); E. H. Lieb and D. C. Mattis, J. Math. Phys. **3**, 749 (1962).

[33] E. H. Lieb, T. D. Schultz, and D. C. Mattis, Ann. Phys. **16**, 407 (1961).

[34] J. Richter, N. B. Ivanov, and K. Retzlaff, Europhys. Lett. **25**, 545 (1994).

[35] I. McCulloch, arXiv:0804.2509 (unpublished).

[36] G. Vidal, Phys. Rev. Lett. **98**, 070201 (2007).

[37] F. Pollmann, S. Mukerjee, A. M. Turner, and J. E. Moore, Phys. Rev. Lett. **102**, 255701 (2009).

[38] F. Verstraete and J. I. Cirac, arXiv:cond-mat/0407066 (unpublished); F. Verstraete, M. M. Wolf, D. Perez-Garcia, and J. I. Cirac, Phys. Rev. Lett. **96**, 220601 (2006).

[39] V. Murg, F. Verstraete, and J. I. Cirac, Phys. Rev. B **79**, 195119 (2009).

[40] G. Refael and J. E. Moore, Phys. Rev. Lett. **93**, 260602 (2004).

[41] H. Tran and N. E. Bonesteel, arXiv:0909.0038 (unpublished).

[42] V. Pasquier and H. Saleur, Nucl. Phys. B **330**, 523 (1990).

[43] M. Oshikawa, D. Schwandt, and F. Alet (unpublished).